



**HAL**  
open science

## Comparison of environmental forcings affecting suspended sediments variability in two macrotidal, highly-turbid estuaries

Isabel Jalon Rojas, Sabine Schmidt, Aldo Sottolichio

► **To cite this version:**

Isabel Jalon Rojas, Sabine Schmidt, Aldo Sottolichio. Comparison of environmental forcings affecting suspended sediments variability in two macrotidal, highly-turbid estuaries. *Estuarine, Coastal and Shelf Science*, 2017, 198, pp.529-541. 10.1016/j.ecss.2017.02.017 . hal-04600751

**HAL Id: hal-04600751**

**<https://hal.science/hal-04600751v1>**

Submitted on 4 Jun 2024

**HAL** is a multi-disciplinary open access archive for the deposit and dissemination of scientific research documents, whether they are published or not. The documents may come from teaching and research institutions in France or abroad, or from public or private research centers.

L'archive ouverte pluridisciplinaire **HAL**, est destinée au dépôt et à la diffusion de documents scientifiques de niveau recherche, publiés ou non, émanant des établissements d'enseignement et de recherche français ou étrangers, des laboratoires publics ou privés.



Distributed under a Creative Commons Attribution - NonCommercial - NoDerivatives 4.0  
International License

# ACCEPTED MANUSCRIPT

## **Comparison of environmental forcings affecting turbidity variability in two macrotidal, highly-turbid estuaries.**

Jalón-Rojas, I., Schmidt, S., and Sottolichio, A.

### **DOI**

<https://doi.org/10.1016/j.ecss.2017.02.017>

### **Publication date**

2017

### **Document version**

Accepted author manuscript

### **Published in**

Estuarine, Coastal and Shelf Science

### **Citation**

Jalón-Rojas, I., Schmidt, S., and Sottolichio, A. (2017). Comparison of environmental forcings affecting turbidity variability in two macrotidal, highly-turbid estuaries. *Estuar. Coast. Shelf Sci.* 158, 529-541, doi: 10.1016/j.ecss.2017.02.017.

### **Important note**

This is a PDF file of an unedited manuscript that has been accepted for publication. To cite this publication, please use the final published version (if applicable).

Please check the document version above in the following link:

<https://www.sciencedirect.com/science/article/pii/S0272771417301750?via%3Dihub>



This version of the accepted manuscript has been prepared according to the sharing policies of Elsevier: <https://www.elsevier.com/about/policies/sharing>

# Comparison of environmental forcings affecting suspended sediments variability in two macrotidal, highly-turbid estuaries

Isabel Jalón-Rojas<sup>1</sup>, Sabine Schmidt<sup>2</sup>, Aldo Sottolichio<sup>1</sup>

<sup>1</sup> Univ. Bordeaux, EPOC, UMR5805, F33600 Pessac, France

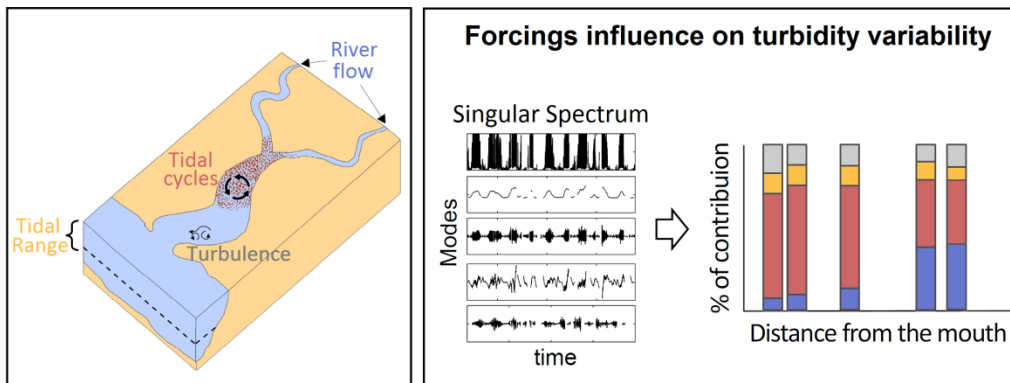
<sup>2</sup> CNRS, EPOC, UMR5805, F33600 Pessac, France

**Corresponding author:** Isabel Jalón-Rojas (isabel.jalon-rojas@u-bordeaux.fr)

## Abstract

The relative contribution of environmental forcing frequencies on turbidity variability is, for the first time, quantified at seasonal and multiannual time scales in tidal estuarine systems. With a decade of high-frequency, multi-site turbidity monitoring, the two nearby, macrotidal and highly-turbid Gironde and Loire estuaries (west France) are excellent natural laboratories for this purpose. Singular Spectrum Analyses, combined with Lomb-Scargle periodograms and Wavelet Transforms, were applied to the continuous multiannual turbidity time series. Frequencies of the main environmental factors affecting turbidity were identified: hydrological regime (high versus low river discharges), river flow variability, tidal range, tidal cycles, and turbulence. Their relative influences show similar patterns in both estuaries and depend on the estuarine region (lower or upper estuary) and the time scale (multiannual or seasonal). On the multiannual time scale, the relative contribution of tidal frequencies (tidal cycles and range) to turbidity variability decreases up-estuary from 68% to 47%, while the influence of river flow frequencies increases from 3% to 42%. On the seasonal time scale, the relative influence of forcings frequencies remains almost constant in the lower estuary, dominated by tidal frequencies (60% and 30% for tidal cycles and tidal range, respectively); in the upper reaches, it is variable depending on hydrological regime, even if tidal frequencies are responsible for up to 50% of turbidity variance. These quantifications show the potential of combined spectral analyses to compare the behavior of suspended sediment in tidal estuaries throughout the world and to evaluate long-term changes in environmental forcings, especially in a context of global change. The relevance of this approach to compare nearby and overseas systems and to support management strategies is discussed (e.g., selection of effective operation frequencies/regions, prediction of the most affected regions by the implementation of operational management plans).

## Graphical Abstract



**Keywords:** turbidity; time series; estuaries; spectral analysis; discharge-turbidity interaction; tide-turbidity interaction

### Highlights:

- First quantification of factors affecting turbidity variability along estuary axis.
- The impact of forcings frequencies is classified by the estuarine region and the time scale.
- Two tidal estuaries are compared revealing similar trends in environmental forcing.
- Common patterns on tidal estuaries throughout the world are highlighted.

## 1. Introduction

Dynamics of estuarine suspended particulate matter (SPM) are complex and strongly variable over time scales ranging from seconds to years. SPM distribution in the water column results from the balance between erosion, transport and deposition processes, which are modulated by the combination of multiple controlling forces (Dyer, 1988). Understanding the variability of SPM requires a good knowledge of these forcings and of their interactions at all the significant time scales. In tidal estuaries, the analysis of factors influencing fine sediment dynamics is often related to the identification of mechanisms causing turbidity maximum zones (TMZ; Allen et al., 1980; Dyer, 1988; Talke et al., 2009). Subsequently, most works have mainly addressed the response of the TMZs to changes of the main forcings, such as river flow and tidal range (Uncles & Stephens 1993; Fettweis et al., 1998; Grabemann et al., 1997; Uncles et al., 2006; Jalón-Rojas et al., 2015, 2016b).

The identification of environmental factors affecting turbidity rarely includes a consistent evaluation of their relative contribution to SPM variability that considers the spatial and temporal dimensions. These latter aspects are particularly important as estuaries are dynamic ecosystems where environmental forcings are not in steady state but evolve under the effect of climate change (Pugh, 2004; Alfieri et al., 2015) and human activities (Winterwerp and Wang., 2013; Uncles et al., 2013). Knowing the influence of forcings in different regions of an estuary is imperative to better understand the behavior of these systems, but also to anticipate their response to environmental changes or human interventions. The quantification of the forcings influence with time is a key issue prior to any evaluation of the response of estuarine systems to long-term changes.

Environmental forcings affecting SPM in coastal systems are relatively well known. They involve deterministic (tidal cycles, tidal range) and stochastic (river flow, wind, turbulence) components (Schmitt et al., 2008) that result in multiscale, non-stationary and nonlinear dynamics. Quantifying the contribution of each forcing to turbidity variability is then a complex task that has been barely explored. Two studies carried out in the San Francisco Bay and the Blyth Estuary (Schoellhamer et al., 2002; French et al. 2008) quantified turbidity variability at time scales related to environmental forcings. In both cases, Singular Spectrum Analysis (SSA; Schoellhamer, 2001) was applied to high-frequency SPM concentration time series, but these analyses were spatially limited to a single cross section of each system. The scarcity of long-term high-frequency time series is probably responsible for the lack of such quantitative analysis. In fact, long-term, multi-site SPM monitoring requires substantial effort and is still not very common in estuaries (Jalon-Rojas et al., 2016).

The Gironde and Loire estuaries are quite unique in having a continuous monitoring of turbidity for about a decade. These macrotidal and highly-turbid estuaries are geographically very close and drain the two main French watersheds to the Bay of Biscay. A well-developed TMZ, characterized by SPM concentrations higher than  $1 \text{ g l}^{-1}$  in surface waters, is a well-known feature in the Loire (Gallene 1974; Jalón-Rojas et al., 2016b) and in the Gironde (Allen and Castaing, 1973; Jalón-Rojas et al., 2015). Thanks to high frequency monitoring, the SPM dynamics are now well documented in these two estuaries, from intratidal to interannual time-scales (Jalón-Rojas et al. 2015, 2016b). The Gironde and the Loire estuaries are then two excellent natural laboratories to evaluate the relative impact of forcings on SPM. Furthermore, the comparison of these two nearby estuaries is of great interest in order to further understand the common behavior of suspended sediments.

The objective of this work is to quantify the turbidity variability at time scales characteristic of environmental forcings in macrotidal estuaries. For this purpose, we combine different spectral methods to analyze the high-frequency multiannual turbidity time series recorded in the Gironde and the Loire estuaries. The specific aim is to estimate and compare the relative contributions of the main

identified forcings frequencies on turbidity at seasonal and multiannual time scales and in different estuarine regions of these two estuaries. This approach allow: (a) to detail the variability time scales of turbidity beyond the classical qualitative analysis; and (b) to compare patterns in nearby, but also distant overseas, tidal systems; and (c) to evaluate the consequences of changes in forcings on turbidity variability.

## 2. The study sites

The Loire and the Gironde are two macrotidal fluvial-estuarine systems located on the Atlantic French coast (Fig. 1). Their main morphological and hydrological characteristics are summarized in Table 1.

With respective surface areas of 635 km<sup>2</sup> and 102 km<sup>2</sup>, the Gironde and the Loire estuaries are the two largest French estuaries. The Loire has a single riverine channel showing a funnel-shape in the outer estuary (Fig. 1.A). The mean depth of its navigation channel, which is permanently dredged, is about 5.5 m between Donges and Trentemoult (Table 1, Cheviet et al., 2002). The Gironde Estuary is funnel-shaped between the mouth and the junction of two tidal rivers (the Garonne and the Dordogne Rivers, Fig. 1.B). Downstream the junction, the estuary has two main channels separated by elongated sand banks and shoals. The left bank channel is permanently dredged for navigation to maintain a minimum depth of 8m at low tide. The right-bank channel evolves naturally and presents a mean depth of about 5m.

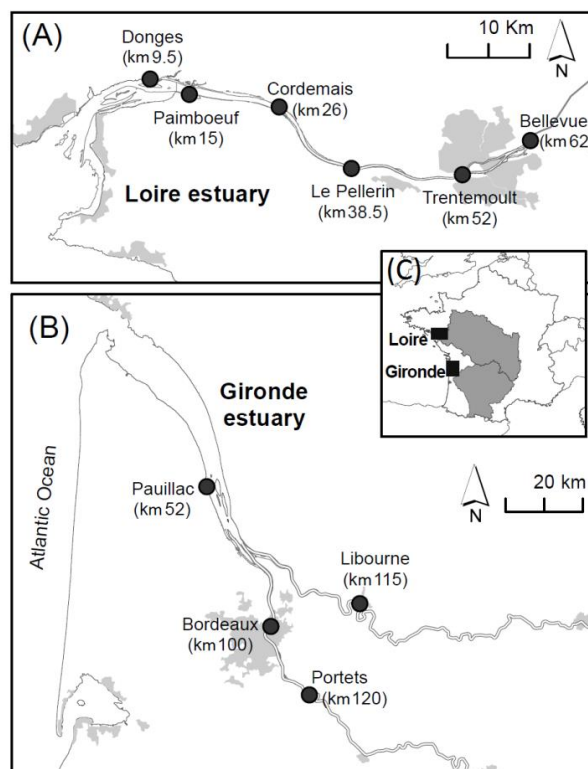


**Figure 1.** Maps of the (A) Loire and (B) Gironde estuaries. Black circles locate the measuring stations. Light gray areas show urban zones. (C) Location maps of the two estuaries (Atlantic French coast); gray areas show the respective watersheds. The number in bracket corresponds to the distance, in km, of each station from the mouth.

Tides are semidiurnal and have similar tidal ranges at the two mouths (Table 1). The tidal waves propagate up to 100 km and 180 km from the mouth in the Loire and the Gironde, respectively, where they are completely damped by friction. During their upstream propagation, tides become increasingly asymmetrical (flood shorter than ebb) and the wave is amplified (Allen et al., 1980; Le Hir and Thouvenin, 1994). The highest tidal range, about 6.3 m, is reached between 26 and 52 km (from the mouth) for the Loire (Jalón-Rojas et al., 2016b) and between 100 and 126 km for the Gironde (Castaing et al., 2006) (Table 1). The tidal wave starts to damp around 52 and 130 km (from the mouth) for the Loire and Gironde, respectively.

Feature	Loire	Gironde
Length	100 km	180 km
Surface	102 km <sup>2</sup>	635 km <sup>2</sup>
Channel depth	5.5 m (Donges-Trentemoult) 14 m (St. Nazaire-Donges)	5 m (Right channel) 8 m (Left channel)
Tidal Range (mouth) <sup>1</sup>		
Mean neap tide <sup>2</sup>	2.9 m	2.2 m
Mean spring tide	4.6 m	4.3 m
Maximal tidal wave		
Km from mouth	26 - 52	100-126
Maximum Tidal Range	6.36 m	6.3 m
Watershed		
Surface	118 000 km <sup>2</sup>	81 000 km <sup>2</sup>
Reservoir total volume	447 hm <sup>3</sup>	2167 hm <sup>3</sup>
Daily River flow <sup>1</sup>		Garonne (60%)+Dordogne(40%)
Min	103 m <sup>3</sup> s <sup>-1</sup>	104 m <sup>3</sup> s <sup>-1</sup>
Mean	775 m <sup>3</sup> s <sup>-1</sup>	684 m <sup>3</sup> s <sup>-1</sup>
Max	3980 m <sup>3</sup> s <sup>-1</sup>	6048 m <sup>3</sup> s <sup>-1</sup>
Summer-averaged	341 m <sup>3</sup> s <sup>-1</sup>	296 m <sup>3</sup> s <sup>-1</sup>
Winter-averaged	1389 m <sup>3</sup> s <sup>-1</sup>	1003 m <sup>3</sup> s <sup>-1</sup>
Annual river flow		
Min	425 m <sup>3</sup> s <sup>-1</sup> (2011)	433 m <sup>3</sup> s <sup>-1</sup> (2011)
Mean	860 m <sup>3</sup> s <sup>-1</sup>	680 m <sup>3</sup> s <sup>-1</sup>
Max	1128 m <sup>3</sup> s <sup>-1</sup> (2013)	961 m <sup>3</sup> s <sup>-1</sup> (2013)

<sup>1</sup> Values were calculated for the periods corresponding to the time series: from 2005 to 2014 for the Gironde and from 2007 to 2014 for the Loire. Daily river flows are from the French national discharge database.

<sup>2</sup> Spring and neap tides were defined as the tidal cycles for which tidal range is respectively above the 75th percentile and below the 25th percentile.

**Table 1.** Main characteristics of the Loire and the Gironde estuaries.

The Loire and the Gironde drain the two largest French watersheds, covering together one third of the French territory (Figure 1.C, Table 1). The Loire daily-mean discharge is equivalent to the sum of the Garonne and Dordogne inputs to the Gironde (Table 1). In both estuaries the minimum and maximum values are measured during the periods comprised between July-September and December-February, respectively. In addition, the Garonne River has a second period of high river discharge between April and May due to snow melting in the Pyrenees. Over the last decade, the driest and wettest years were 2011 and 2013, respectively. There are water abstractions in both watersheds, particularly to sustain

discharge during summer, but the Garonne and the Dordogne Rivers have the highest number of reservoirs and a storage capacity about five times higher than that of the Loire (Table 1). The variability in hydrology over the last decades is quite similar for the Gironde and the Loire (Chevalier et al., 2014). These watersheds show a trend in decreasing river flow induced by climate change and land use (Boé et al., 2009).

In both systems, the asymmetry of the tidal wave, when propagating upstream, coupled to density residual circulation creates a pronounced TMZ (suspended sediment concentrations  $> 1 \text{ g l}^{-1}$ , Allen et al., 1980). The Gironde estuary is known for a naturally well-developed TMZ (Castaing and Allen, 1981), even if there is no fully reliable reference state before the 1970's.. For the Loire estuary, there is evidence that its current hyperturbid state was more recently reached, largely due to continuous artificial modifications of its morphology during the last two centuries, which progressively favored the flood-dominant conditions (Winterwerp and Wang, 2013). One could refer to Jalón-Rojas et al., (2015; 2016b) for a detailed description of turbidity and TMZ dynamics from tidal to multi-annual time scales in the Gironde and the Loire estuaries.

### **3. Materials and Methods**

#### **3.1. The monitoring systems**

The Loire and the Gironde estuaries have each an automated, high-frequency, long-term monitoring network of water quality, called SYVEL (SYstème de Veille dans l'Estuaire de la Loire) and MAGEST (MAREL Gironde ESTuary), respectively. SYVEL includes six stations distributed from the mouth up to 62 km upstream (Figure 1.A). This network was implemented in 2007, except the station of Donges that was added in December 2010. Cordemais station was stopped in December 2011. It must be noted that the station of Paimboeuf is situated in a particularly shallow area, which could introduce a bias in turbidity levels. Implemented in 2005, the MAGEST network consisted initially of four stations: one in the central estuary, one in the Dordogne tidal river and two in the Garonne tidal river (Figure 1.B). Portets station was stopped in January 2012. All the stations measure dissolved oxygen, salinity, temperature and turbidity at 1m below the surface. Except the station of Bellevue in the Loire, the sites are equipped with real-time autonomous monitoring systems (see Etcheber et al., 2011 for details). The turbidity sensor (Endress and Hauser, CUS31-W2A) records values between 0 and 9999 NTU every 10 minutes (every 60 minutes for Cordemais in the Loire). The saturation value (9999 NTU) corresponds to  $5\text{-}6 \text{ g l}^{-1}$  (Schmidt et al, 2014; GIP Loire Estuaire, 2014). Bellevue station is equipped with a SMATCH multiparameter sensor, whose turbidimeter has the same response than the CUS31-W2A sensor in the 0-2000 NTU range encountered in the upper Loire estuary (Jalón-Rojas et al., 2016b). The time series used in the present work start in January 2005 for the Gironde, and in January 2007 for the Loire. They include data until July 2014 in both systems. The rates of correct operating during these periods were: 71% (Bordeaux), 70% (Portets), 70% (Libourne) and 57% (Pauillac) for the Gironde; 94.5% (Donges), 80% (Paimboeuf), 80% (Cordomais), 80.5% (Le Pellerin), 84% (Trentemoult) and 90% (Bellevue) for the Loire. Daily river flows of the Loire, Garonne and Dordogne Rivers are provided by the French national discharge database ([www.hydro.eaufrance.fr](http://www.hydro.eaufrance.fr)).

#### **3.2. Data treatment: spectral analysis**

Turbidity time series were analyzed using the Singular Spectrum Analysis (SSA) combined with the Lomb-Scargle periodogram (LSP) for the multiannual analysis, and by the Continuous Wavelet



Transform (CWT) for the seasonal analysis. This strategy is based on a recent work (Jalón-Rojas et al., 2016a) that tested and compared the performance of the different spectral techniques mostly used in coastal research for the analysis of high-frequency, long-term time series of physico-chemical parameters. Using turbidity time series as an example, this work evaluated the limits of each method for different rates and two distributions of missing data, and their capacity to quantify the contribution of environmental forcings to the variability of the studied parameter, among others. Here we describe briefly the different spectral methods applied in this work; see Jalón-Rojas et al. (2016a) for details.

### **3.2.1. Singular Spectrum Analysis (SSA)**

The SSA decomposes time series into a sum of nearly periodic time series, the so-called reconstructed components (RCs) (Vautard et al., 1992; Schoellhamer, 1996). It is based on the principle of sliding a window of width  $M$  down a time series to obtain an autocorrelation matrix. Except one or two RCs that have characteristic frequencies higher than  $M$ , RCs contain variation in the time series with periodicities between  $0.2M$ — $M$ . The contribution of each RC to the variance is given by its corresponding eigenvalue ( $\lambda$ ). Most of the variance is contained in the first RCs. The representation of  $\lambda$  in order of decreasing magnitude exhibits a steep initial slope containing the significant components, which is followed by a mild slope that represents the noise level. The reader is referred to Vautard et al. (1992), Ghil et al. (2002) and Schoellhamer et al. (2011) for detailed descriptions.

Here we use the algorithm proposed by Schoellhamer (2001) for time series with missing data. SSA recognizes the main variability at frequencies that can be related to known forcings frequencies. SSA properly estimates their contribution to the parameters variability even with 70% missing data (Jalón-Rojas et al., 2016a). The contribution of forcings could be slightly underestimated, up to -5%, for shortened time series (Jalón-Rojas et al., 2016a). This potential bias is taken into account for the stations whose time series are the shortest (Donges, Cordemais and Portets).

SSA is applied in two steps. Firstly, SSA is applied to the 10-min time series with a window size of 25-h, i.e.,  $M=150$  as turbidity is collected every 10 min (except for Cordemais, where  $M=25$  since recording time step is 60 min). The result is formed by a single RC for the total subtidal variability, and the rest of RCs representing different intratidal time scales. Secondly, SSA is applied to tidally averaged turbidity time series with a window size of 1250-h ( $M=100$ , time step of 12.5 hours), obtaining several RCs that contain different subtidal variability time scales. The contributions ( $\lambda$ ) to the total variance of RCs from the second step are pondered by the weight  $\lambda$  of subtidal RC calculated in the first step. The reader is referred to Schoellhamer (2002) for a detailed description of the application of SSA in several time steps.

### **3.2.2. Lomb-Scargle Periodogram (LSP)**

The LSP (Lomb, 1976; Scargle, 1982) decomposes time series into periodicities and identifies the most energetic ones. Based on harmonic regression, it consists on a least-squares power spectrum that is applicable to irregularly sampled data. LSP was widely promoted by Press et al. (1992), who developed an optimized algorithm. We use the Press's algorithm implemented in MATLAB by Brett Shoelson, which provides significance levels to select the main variability time scales.

The LSP method is able to detect periodical forcings, even with 70% missing data, but is less suitable for evaluating non-periodic factors and long-term trends (Jalón-Rojas et al., 2016a). In addition, it does not allow time-varying analysis. LSP appears then less efficient compared to SSA, but can give complementary information. It is a complementary method of SSA for calculating the characteristic frequency of the unequally sampled RCs because of its high efficiency with incomplete time series.

Furthermore, the power law of the spectrum trend ( $E(f) \approx f^{-\beta}$ ) provides scaling properties of variables (Schmitt et al., 2008; Derot et al., 2015): i.e., the scaling exponent  $\beta$  is equal to 0 for noise, 2 for Brownian motion and 5/3 for turbulence.

### 3.2.3. The Continuous Wavelet Transform (CWT)

Wavelet spectra are time-varying periodograms that provide both the dominant variability time scales and their energetic variability over time. In this work we apply the continuous wavelet transform (CWT) with the Morlet function, which is appropriate for coastal time series (Daebechies, 1992; Farge 1992). The CWT is used to decompose the signal into a weighted sum of small waves that are obtained by translation and dilation of a reference wavelet (the Morlet function in this case). A complete guide on Morlet wavelets and their applications is provided by Torrence and Compo (1998). The main limitation of CWT is the need of regularly sampled data. Therefore it can only be applied to short continuous datasets from the original discontinuous time series. Whereas SSA is advantageous in the quantification of forcings, CWT offers a visual and interpretable representation of their temporal variation. The combination of both methods results in a meaningful method for analyzing continuous datasets (Jalón-Rojas et al., 2016a). Here we use the wavelet algorithm developed and implemented in MATLAB by Grinsted et al. (2004).

## 4. Results

### 4.1. Times scales of turbidity variability

Turbidity time series of the Gironde (10-years) and Loire (7-years) estuaries reveal marked multiscale variability, with ranges of values between 10 and 9999 NTU. When the TMZ is present, tidally averaged turbidity reaches values up to 3500 NTU in the central Gironde estuary (Pauillac) and up to 7500 NTU in its upper reaches (Bordeaux and Libourne). In the Loire, tidally averaged turbidity reaches up to about 3900 NTU (Donges) and 8800 NTU (Cordemais) in the lower and central reaches. In the uppermost stations, it always remains below 3000 NTU, 1550 NTU, and 500 NTU at Le Pellerin, Trentemoult and Bellevue, respectively. Turbidity trends in these two estuaries are described in Jalón-Rojas et al. (2015, 2016b).

In this work, we have selected two time series recorded in the upper Loire (Le Pellerin station) and the upper Gironde (Bordeaux station) in order to illustrate and compare the different scales of variability and their driving factors:

- semidiurnal tidal cycles: turbidity varies during the semidiurnal tide following deposition-resuspension-advection cycles induced by changes in current velocities (Fig. 2.A, Castaing and Allen, 1981; Grabeman et al., 1989).
- fortnightly tidal cycles: turbidity (values and range) increases from neap to spring tides with increasing currents velocities that favour shear bed stress and vertical mixing (Fig. 2.B, Allen et al., 1980);
- seasonal timescale: the decreases of river flow, usually in summer, promotes the upstream migration of the TMZ and thus the increase of turbidity in the upper reaches (Fig. 2.C)
- interannual variability: turbidity is higher during dry years, as in 2011, and lower during wet years, as in 2013. This pattern is common to both estuaries, although less visible in Bordeaux where raw data

reach the saturation value even during wet summers (figs. 2.D.I and 2.D.2). Higher river flows are more efficient in flushing the TMZ to lower estuarine regions (Jalón-Rojas et al., 2015).

The hydrodynamic factors were not directly recorded, but they can be reasonably linked to a time scale of variability. Therefore it can be hypothesized that the relative contribution of a given frequency is an indicator of the relative contribution of its associated forcing to the SPM variability.

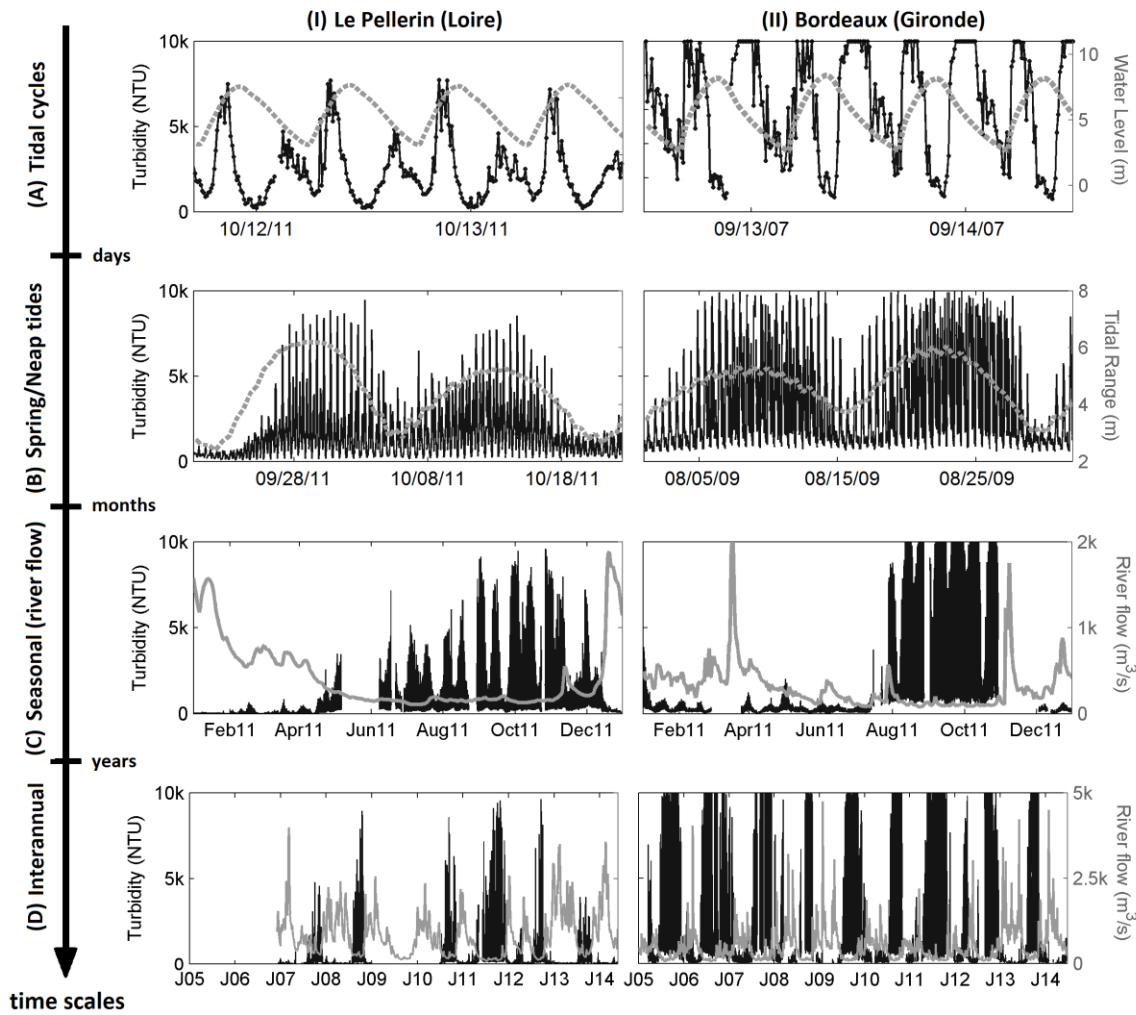


**Figure 2.** Turbidity (black lines) time series at Le Pellerin (I, Loire) and Bordeaux (II, Gironde). Turbidity time series are detailed considering semidiurnal (A), fortnightly (B) seasonal (C), and multi-annual (D) time scales. For each time scale, turbidity is plotted along with the most relevant driving parameter (water level, tidal range and river flow; gray lines) to highlight changes.

#### 4.2. Spectral quantification of forcings contributions

The simple description of the time series highlights that turbidity varies significantly under the effect of tides and river flow, which appear as the two main factors affecting SPM variability in the Gironde and Loire estuaries. Awkwardly, these two forcings induce turbidity variations of similar order of magnitude: it is then difficult to compare their relative influences in different estuarine regions and between different estuaries only through descriptive methods. The application of SSA to time series

allows to characterize all the significant time scales of turbidity variability and the associated forcings in a more rigorous way than that obtained by a qualitative interpretation (Section 4.1 or other studies such as Mitchell et al., 2012). However, the main interest of spectral analyses is to permit the determination of their relative contribution to the total variability. In addition, the Lomb-Scargle periodograms were plotted in order to scale properties of turbidity through the power spectral slopes and to compare the significant time scales of variability to those obtained from SSA. Figures 3 and 4 illustrate the Lomb Scargle periodogram and the SSA decomposition of the turbidity time series applied to Le Pellerin (Loire Estuary).

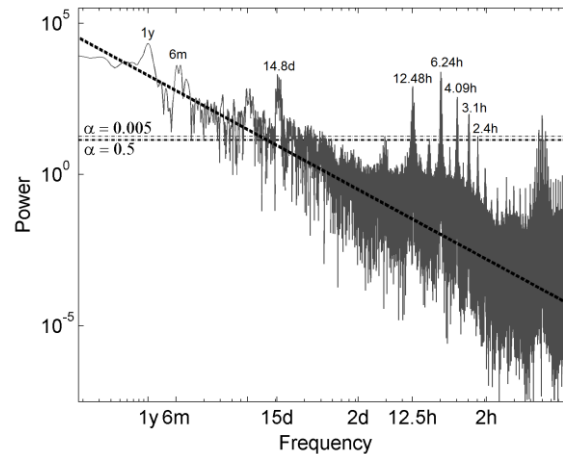


**Figure 3.** Lomb-Scargle periodogram of the turbidity time series at Le Pellerin (Loire). Horizontal dotted gray lines correspond to the significance levels ( $\alpha$ ) of 0.005 and 0.5. Dark dotted line represents the power law of turbulence:  $E(f) \approx f^{-5/3}$ .

Using SSA method, turbidity time series were decomposed into five significant modes (RCs, Fig. 4). Once identified, each RC or group of RCs is assigned to an environmental forcing frequency. Turbidity modes with variability time scales of 12.4h, 6.21h, 4.09h, 3.1h and 2.48 were grouped in the RC1 which is associated to tidal cycles. Semimonthly and monthly turbidity variability induced by tidal range is represented by RC3 and RC5 respectively. All these periodical frequencies were also identified as significant by the LSP (Figure 3).

Due to their multiscale behavior, RC2 and RC4 modes are more difficult to assign to a specific forcing frequency. The detailed description of turbidity in Section 4.1 suggests river discharge as a key parameter. To have a critical assessment of this statement, SSA was applied to river flow time series. Figure 5 compares RC2 of turbidity with RC1 of river flow (A.1 and B.1) and RC4 of turbidity with RC2 of river flow (A.2 and B.2) for a station of the lower Loire estuary (Paimboeuf, A) and a station of the upper Loire estuary (Le Pellerin, B). RC2 modes of turbidity display opposite trend to RC1 modes of river flow as their amplitudes vary in accordance, while trends and amplitudes of turbidity RC4 modes and river flow RC2 modes are similar. Although the previous knowledge of forcings can be helpful to interpret modes, this treatment sustains that RC2 can be assigned to changes in hydrological regime (changes between high and low fluvial discharge): an increase of river flow is accompanied by an increase of turbidity in lower reaches and a decrease in upper reaches. RC4 corresponds thus to river discharge fluctuations.

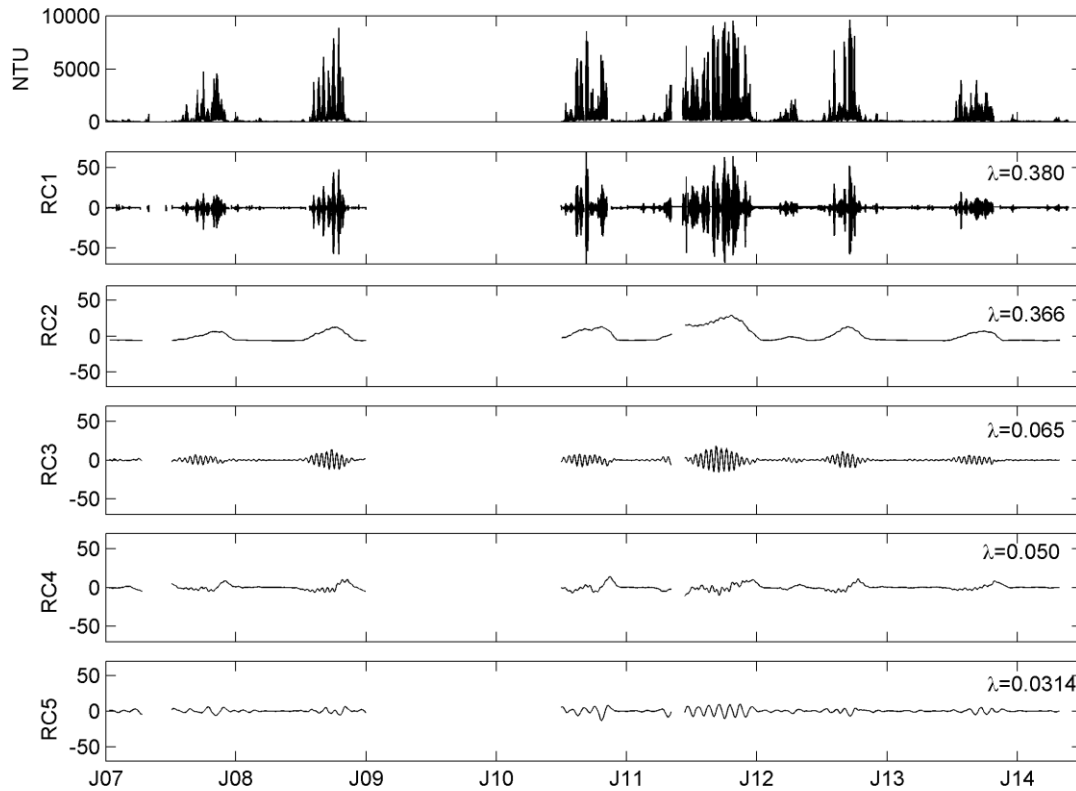


**Figure 4.** Singular spectrum analysis (SSA) of the turbidity time series at Le Pellerin (Loire, January 2007 - July 2014). Forcings associated to each RC are: tidal cycles (RC1), hydrological regime (RC2), tidal range (semimonthly variability) (RC3), river discharge variability (RC4), and tidal range (monthly variability) (RC5).  $\lambda$  is the contribution of each RC to the total turbidity variability.

As introduced in the method section, an interest of SSA is to permit the estimation of the contribution ( $\lambda$ ) of each mode to the total turbidity variance. This analysis thus quantifies the relative contribution of different forcing frequencies, which can be used as indicator of the relative influence of their associated forcings to turbidity variability. In the case of Le Pellerin station (Fig. 4), the hydrological regime (RC2) explains 37% of the variance. Together with the contribution of discharge variability (RC4, 5%), river flow contains 42% of the turbidity variance, being the main forcing at this station, located in the upper Loire estuary. Tidal cycles (RC1) contribute to 38% of the turbidity variance at Le Pellerin. Tidal range represents only 9.5% of the variability at the semimonthly (RC3; 6.5%) and monthly (RC5; 3%) time scales. The five significant modes contain 89.5% of the variance. The Lomb-Scargle periodogram follows a power law curve (Figure 3), whose slope corresponds to the passive scalar of turbulence ( $\beta=5/3$ ). This reveals the turbulent-like behavior of turbidity on time scales ranging from 10 min to 1 year as previously reported by Schmitt (2008). This turbulent behavior is observed at all the stations in both systems (see the LSP of the turbidity time series of Bordeaux in Jalón-Rojas et al., 2016a). This observation suggests that the part of the remaining variance (10.5%) not explained by SSA, might be explained by turbulence together with other unquantifiable processes such as wind, boat traffic. As described above and in section 3.2, spectral analyses were applied to each turbidity times series recorded in the Gironde and the Loire estuaries. We do not intend to present in details the results of each station, that are comparable to those presented for Le Pellerin. The following discussion is focused on the synthesis of these analyses, whose objective is to compare the relative contributions of the main forcing: (a) at seasonal and multiannual time scales; and (b) in different regions of these two estuaries.

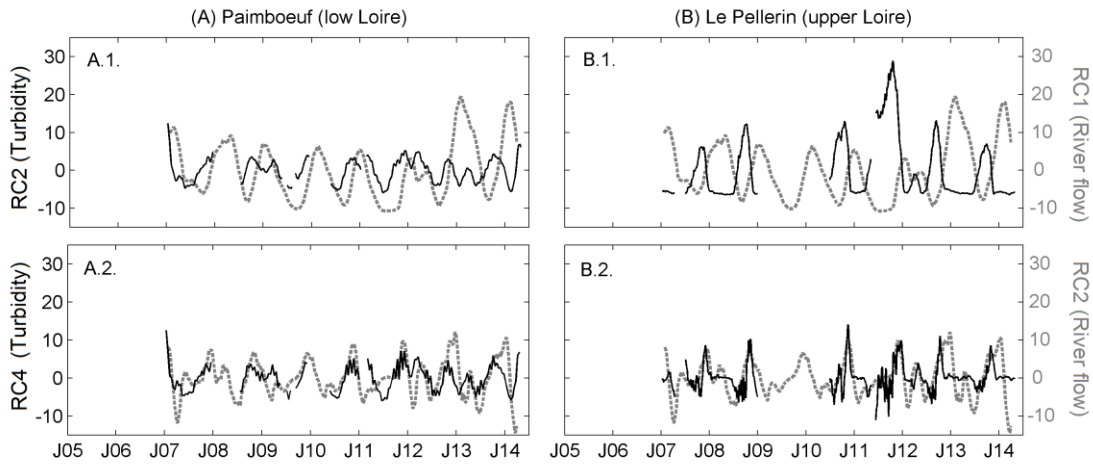


**Figure 5.** Comparison of RC2 (A.1, B.1) and RC4 (A.2, B.2) turbidity modes (black lines) with RC1 and RC2 river flow modes (dashed gray lines) at: (A) Paimboeuf (lower Loire estuary); (B) Le Pellerin (upper Loire estuary).

## 5. Discussion

### 5.1. Multiannual influence of environmental forcings

Not surprisingly, tidal cycles, tidal range and river flow contribute to turbidity variability in the two estuaries of the north Atlantic coast. To deepen the understanding of this dynamic, SSA results are now discussed to test our working hypothesis that their degree of influence varies depending on the considered timescales and estuarine region. First, the relative contributions of forcing frequencies at each station of the Loire and the Gironde estuaries are detailed on multiannual time scale (Fig. 6.A and 6.B). In order to compare the two systems, the contributions of forcings frequencies are also represented as a function of the distance from the mouth normalized by the total length of the estuary (*Position*, Fig. 6.C).

Except for Paimboeuf, the influence of tidal cycles decreases up-estuary in both estuaries. The singularity at Paimboeuf could be explained by its location in shallower water, which exacerbates the change in SPM due to resuspension and deposition cycles. The total contribution of tidal cycles to turbidity variability is 50% in the lower Loire (Donges), 45% in the central Loire (Cordemais) and 37% in the central Gironde (Pauillac). In the upstream sections, it decreases to 38% at Le Pellerin and to 32-34% at Trentemoult, Bordeaux and Portets. The lowest values are reached at Bellevue (29%) and Libourne (26%).

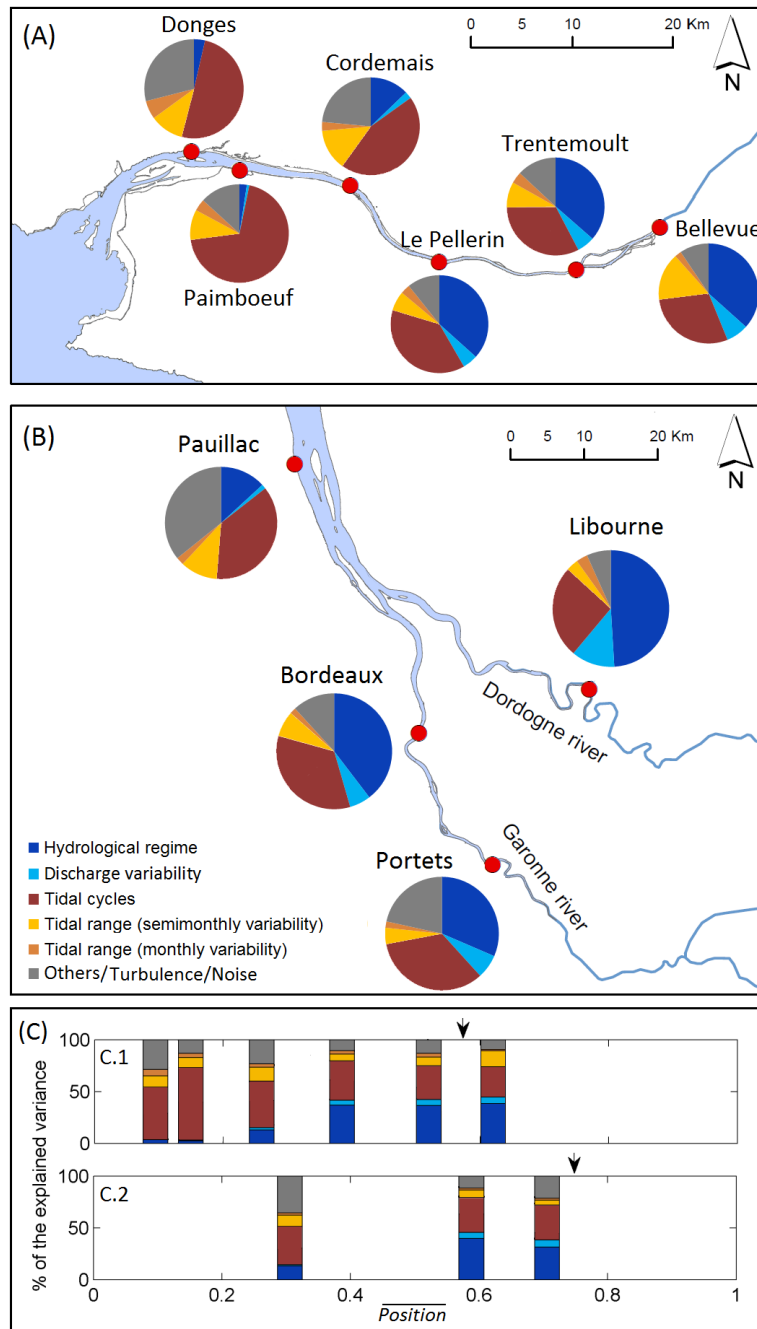


**Figure 6.** Contribution (%) of each forcing to turbidity variability, estimated from the application of SSA to time series of the Loire (A, C.1) and Gironde (B, C.2) estuaries. In (C) the distance from the mouth of each station is normalized by the total length of the corresponding estuary (*Position*) and only the best documented axis of the Gironde (Gironde-Garonne tidal river) is plotted. Arrows indicate the region where tidal range begins to decrease.

On the opposite, the hydrological regime exerts a noticeable higher influence in the upper estuaries. In the Loire, its contribution to the total turbidity variability increases from 2.5% at Donges to 13% at Cordemais, and to about 36% in the three uppermost stations. The Gironde shows similar trends with 13% in the central estuary (Pauillac) and 40% in the tidal Garonne River (Bordeaux). The influence of this forcing in the tidal Dordogne River is even larger (49%). In fact, the ratio of mean turbidity between periods of low (August) and high river (February) discharges is the highest at Libourne (54) compared to Portets (24) and Bordeaux (8) (Jalón-Rojas et al., 2015). Undetectable at Donges, the

influence of river discharge variability, although modest, also increases toward upstream from 1-3% in the central estuaries (Pauillac and Cordemais), to 5-7% in the upper station of the Loire and the Garonne and 12% at Libourne.

Tidal range influence is almost constant along the two estuaries. There is a slight decreasing tendency up-estuary, as observed for tidal cycles, at the opposite to the river flow. Its contribution to turbidity variability is between 13% and 17% in the lower estuaries. In the fluvial Gironde Estuary, it decreases to 9% at Bordeaux and to 6.5% at Portets and Libourne. In the upper Loire, tidal range explains 9.5% at Le Pellerin, but increases slightly in the uppermost stations, particularly at Bellevue (17.5%). This result agrees with the fact that differences of mean turbidity during spring and neap tides are higher at Bellevue (3.6%) than at Le Pellerin (2.2%) during periods of low discharge (Fig. 5 in Jalón-Rojas et al., 2016b). Bellevue is situated in the region where tidal range decays (Figure 6.C.1) and downstream of the TMZ core. Here the availability of sediments depends of the high amounts of sediments that are resuspended during spring tides in the TMZ core and subsequently upstream advected (Fig. 3 in Jalón-Rojas et al., 2016b): tidal range is then an important forcing in this region.

The contributions of river discharge and tides (including tidal cycles and tidal range) to turbidity variability are compared along the longitudinal estuarine axis (Fig. 7). Approximately in the first seaward third of the two estuaries ( $\overline{Position} < 0.35$ ), river discharge contribution increases from about 3% to 42% (Fig. 7.A), and that of tides decreases from about 68% to 47% (Fig. 7.B). In the second third of the estuary ( $0.35 < \overline{Position} < 0.7$ ), both forcings exhibit a similar and almost constant influence. The Gironde and the Loire show a similar present-day tendency, despite the particularities of these two nearby estuaries: two riverine channels in the Gironde, continuous interventions in the Loire's morphology during the last century, and more water storage in the Gironde.

Only two other studies evaluated the influence of environmental forcings on SPM through the SSA of high-frequency time series acquired in the San Francisco Bay-Delta Estuary (USA, Shoellhamer, 2002) and in the Blyth Estuary (UK; French et al. 2008). Unlike the Gironde and the Loire, the San Francisco Bay and the Blyth are mesotidal estuaries with mean spring tides of about 2 m. The San Francisco Bay has a mean-annual river flow of  $600 \text{ m}^3 \text{ s}^{-1}$  equivalent to the two French estuaries (Table 1). By contrast, freshwater inflow of Blyth Estuary is drastically lower ( $0.4 \text{ m}^3 \text{ s}^{-1}$ ). The contributions of tides and river flow on SPM concentrations variability were added in Figure 7, in order to compare these four different estuaries. The influence of both factors in San Francisco Bay agrees with the tendency observed in the Loire and Gironde. However, contrary to the Gironde and the Loire, most of the tidal contribution corresponds to tidal range variability (40% compared with 24% of tidal cycles). This could be explained by the duration of slack waters that varies with the spring-neap cycle in the lower San Francisco Bay (Shoellhamer, 1996, 2001): it is only a few minutes long during spring tides, which is insufficient for a complete deposition of sediments. Consequently, in San Francisco Bay there is no important turbidity variability during the semidiurnal tidal cycle at spring tides, and the tidal range exerts a higher influence on turbidity variability. The lower Blyth Estuary also shows a tidal contribution in agreement with the tendency displayed by the Gironde and the Loire (Fig. 7.B), with a higher contribution of tidal cycles (38.5%) compared to tidal range (28%) (French et al., 2008). However, there is no impact of river discharge due to its negligible level.



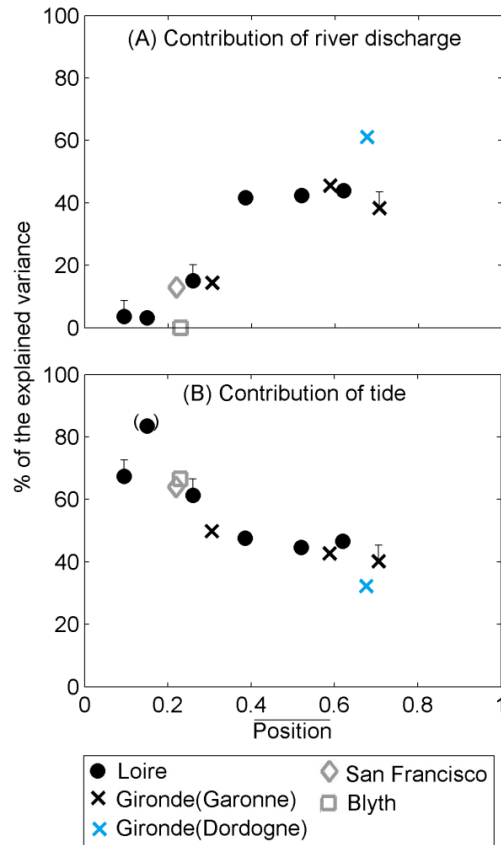


**Figure 7.** Total contributions of river discharge (A, RC1+RC5) and tides (B, RC2+RC3+RC4+RC6) to turbidity variability for the Loire (black circles) and the Gironde (black cross) estuaries. Blue cross represents the station of Libourne (Dordogne River). The parentheses in (B) indicate a possible bias of this value due to the particular location of this station in shallower waters. Error bars are plotted to take into account a potential underestimation in the case of shorter time series (Section 3.2.1). Data from the San Francisco Bay (gray diamonds, Schoellhamer, 2002) and the Blyth Estuary (gray squares, French et al., 2008) are plotted for comparison.

## 5.2. Seasonal changes in forcings influence

RCs time series highlight that the energy of signal oscillation varies over time (e.g. Fig. 4). For example at Le Pellerin, the modes associated to tidal cycles show seasonal variation of energy. This implies that longer timescales can also force variability on the tidal time scale and therefore the relative influence of forcings can vary over time. To investigate more in detail such seasonal changes, we applied the Continuous Wavelet Transform (CWT) combined with SSA to raw datasets of almost continuous turbidity data containing a period of low discharge ( $period_{LD}$ ) followed by a period of high discharge ( $period_{HD}$ ). Figures 8 and 9 illustrate this analysis for datasets of almost 3 months at the lower and upper estuarine regions of the Gironde and the Loire respectively. Wavelet spectrograms evidence that the main variability time scales (associated to tidal cycles and tidal range) have the same temporal evolution of energy during  $period_{LD}$  and  $period_{HD}$  in the lower Gironde (Pauillac station, Fig. 8.B.I) and Loire (Donges station, Fig. 9.B.I). Therefore, the influence of these forcings does not seem to depend on river flow intensity in these regions. On the opposite, there is a clear difference on energy between  $period_{LD}$  and  $period_{HD}$  in the upper Gironde (Fig. 8.B.II) and Loire (Fig. 9.B.II): tidal cycles and range have a lower influence during  $period_{HD}$ . The comparison of the spectrograms reveals that, at an intratidal time scale, turbidity varies mainly at a semidiurnal time scales in the lower Gironde (Fig. 8.B.I) and Loire (Fig. 9.B.I), whereas the importance of other tidal scales is higher in the upper regions of both estuaries (Fig. 8.B.II and Fig. 9.B.II).

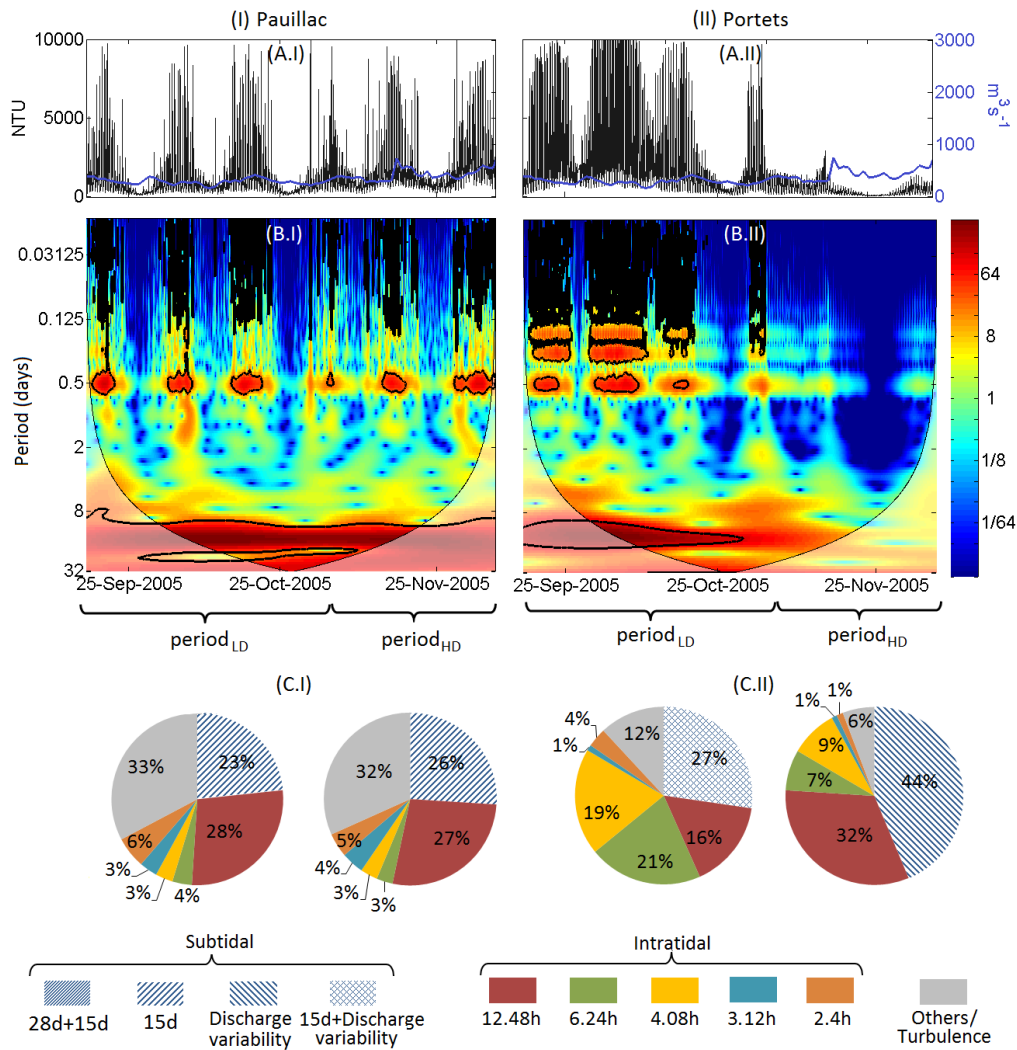


**Figure 8.** (A) Times series of turbidity (black) and river flow (blue) from 16 September to 6 December 2005 at Pauillac (A.I, central Gironde Estuary) and Portets (A.II, upper Gironde Estuary). (B) Corresponding continuous wavelet spectrum of turbidity normalized by the variance (color bar). The thick black contour designates the 5% significance level against red noise. The cone of influence (COI), where edge effects might distort the picture, is shown as a lighter shade. (C) Contribution (%) of the different time scales to the turbidity variability ( $\lambda$ ), calculated from SSA for periods of low and high river discharge. Note that SSA does not differentiate the contribution river flow and spring/neap tidal cycles for 3-month time series.

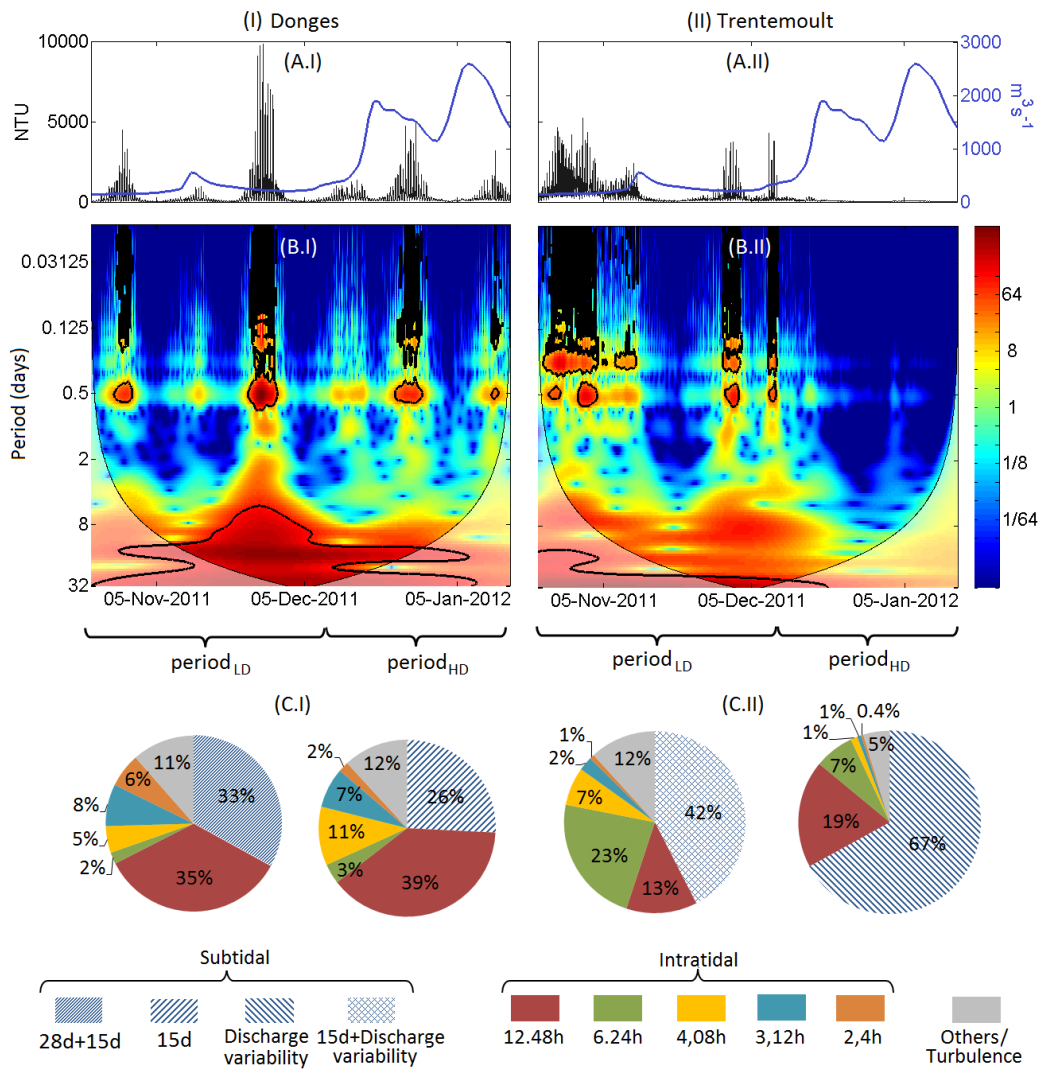


**Figure 9.** (A) Times series of turbidity (black) and river flow (blue) from 22 October 2011 to 15 January 2012 at Donges (A.I, lower Loire Estuary) and Trentemoult (A.II, upper Loire Estuary). (B) Corresponding continuous wavelet spectrum of turbidity normalized by the variance (color bar). The thick black contour designates the 5% significance level against red noise. The cone of influence (COI), where edge effects might distort the picture, is shown as a lighter shade. (C) Contribution (%) of the different time scales to the turbidity variability ( $\lambda$ ), calculated from SSA for periods of low and high river discharge. Note that SSA does not differentiate the contribution river flow and spring/neap tidal cycles for 3-month time series.

To quantify the weight of forcing frequencies on turbidity variability during  $\text{period}_{\text{HD}}$  and  $\text{period}_{\text{LD}}$ , SSA was applied independently to each period to remove the influence of “hydrological regime”. The cut-off point between  $\text{period}_{\text{HD}}$  and  $\text{period}_{\text{LD}}$  was defined from the wavelet spectrograms of the upper stations, at the moment where energy patterns begin to change. This analysis also allows for further discussing the relative importance of the short-term time scales. SSA demonstrates once again that the forcings influence on turbidity is roughly constant in the lower Gironde (Fig. 8.C.I) and Loire (Fig. 9.C.I). Both  $\text{period}_{\text{LD}}$  and  $\text{period}_{\text{HD}}$  exhibit a very similar contribution of tidal cycles (44-42% at Pauillac and 56-62% at Donges) and tidal range (23-26% at Pauillac and 26-33% at Donges). Tidal cycles induce dominantly semidiurnal turbidity variability. In the upper estuaries (Fig. 8.C.II and Fig. 9.C.II), forcings influence is completely different between contrasted hydrological periods. While tidal range is the main subtidal forcing during  $\text{period}_{\text{LD}}$ , river discharge explains the subtidal variability during  $\text{period}_{\text{HD}}$ . In these examples, the subtidal RC of  $\text{period}_{\text{LD}}$  shows a predominant

frequency of 15 days, but also other minor variability frequencies related to river flow since the first small floods were occurring, in particular in Trentemoult (Fig. 9.C.II). Such cyclic changes in tide to river dominance were also described in term of energy by Zhang et al. (2016) for the Yangtze Estuary. Concerning the different time scales of turbidity variability due to of tidal cycles, it is noticeable that there is a higher variability at 6.24 h, but only during period<sub>LD</sub>. The RCs corresponding to 6.24 h show variability peaks at the resuspension phases, slightly higher during flood, suggesting that the core of the TMZ core is centered at these stations.

### **5.3. Grading the impact of main environmental forcings**

This work suggests common patterns in forcings impacts on turbidity variability along tidal estuaries. Such impacts can be classified by estuarine region (lower and upper estuary) and time scale (multiannual and seasonal) (Table 2). On multiannual time scale, turbidity variability in the lower estuary is dominated by tidal cycles (up to 50%), followed by tidal range and then river flow. This region preserves also this classification on the seasonal time scale regardless the range of river discharge. The only difference is that river flow exerts a negligible influence at seasonal time scales as hydrological regime, able to shift the position of the TMZ, are no considered. By contrast, the upper estuary exhibits different patterns depending on the considered time scale. On multiannual scale, turbidity variability is dominated by river flow (41-49%), followed by tidal cycles and tidal range. This pattern is the same for periods of high river flow on seasonal time scales. Even if the hydrological regime is not considered, river flow dominates turbidity variability in upper reaches during wet periods. In contrast, during periods of low river discharge, the upper estuary shows the same trends as observed in the lower estuary since it is dominated by tidal cycles.

		Factor	Lower-estuary (first third)	Upper- estuaries (second third)
Multiannual		Tidal cycles	37-50% +++	29-38% ++
		Tidal range	13-17% ++	10-18% +
		River flow	3-15% +	42-49% +++
		Others/ Turbulence/ Noise	25-36% ++	7-13% +
Seasonal	High discharge	Tidal cycles	+++	++
		Tidal range	++	+
		River flow	0	+++
		Others/ Turbulence/ Noise	++	+
	Low discharge	Tidal cycles	+++	+++
		Tidal range	++	++
		River flow	0	+
		Others/ Turbulence/ Noise	++	++

**Table 2.** Classification of forcings impact on multiannual and seasonal scales. Symbols represent the influence of forcings from negligible (0) to high (+++).

#### 5.4 Implication for management strategies

The management of estuaries present common problems related to dredging, engineering works, port and industry development, water quality, regulation of incoming river flow, etc. (Mitchell et al., 2013). A good knowledge of environmental forcings and of their relative influence is required for management strategies that envisage modifications of such forcings. For example, the low-water management plan in the tidal Garonne river aims to sustain the discharge through the release of stored water in upstream dams during severe low discharge periods in order to limit turbidity and deoxygenation (Schmidt et al., 2016). The present work demonstrates that the impact of such approach will be restricted to the landward reaches up to a distance of around two thirds of the estuary length, where river flow has a significant influence (Fig. 6; Table 2). In addition, if these releases occur only occasionally, it is likely that their effects would be very limited, even null, as shown during period<sub>LD</sub> at Trentemoult where the small flash flood exerted a low influence (Fig. 9.C.II). To obtain significant effects on water quality and to decrease turbidity significantly in the upper estuary, the frequency of water releases should be sustained during seasons of low river flow. This would reduce the variability

due to hydrological regime that, together with discharge variations, influences over 40% of total turbidity variability.

Forcings could be also modified by meteorological and climatological variations (Robins et al., 2016). According to IPCC (2013), climate change is expected to significantly modify mean sea levels, storms, river discharges and sediment supply in estuaries by 2050. These effects result, among others, in tidal modifications and morphological adjustments that in turn influence tidal propagation (Friedrichs and Aubrey, 1988; Chernetsky et al, 2010). The impact of climate change at regional scales is currently a work in progress. In the case of the Loire and Garonne watershed, a decrease in mean river discharges, particularly during summer and fall, is predicted for the middle of the 21st century (Boé et al., 2009). This could introduce to a change of forcings weights: the patterns found for low river discharge periods at upper reaches (Fig. 8.II and 9.II, Table 2) will be more persistent over year. Tides will become the dominant forcings during more time at the expenses of river flow, which will favor the upstream transport of suspended sediments. This can in turn have repercussions for management operations, such as dredging. Just as lower reaches must be dredged throughout the year, the frequency of dredging at upper reaches will increase and even the uppermost limit of dredging could be displaced up-estuary.

Given that forcings, and therefore their impact on suspended sediments, can evolve under the effect of climate change and human interventions, indicators of such evolution are essential. The application of this methodology to future long-term high-frequency time series could allow the evaluation of such evolution. Therefore, we propose the use of the relative contributions of forcings to the variability of physical parameters, such as turbidity, as an indicator of long-term changes of forcings and their impact on such parameters.

## 6. Conclusions

The relative influence of environmental forcing frequencies affecting suspended sediments was evaluated and compared along two nearby, macrotidal, hyper-turbid estuaries: the Gironde and the Loire (west France). For this purpose, Singular Spectrum Analyses, combined with the Lomb-Scargle periodogram and the Wavelet Transform, were applied to the high-frequency, multiannual time series recorded by automated monitoring networks. Six environmental forcing frequencies controlling turbidity variability were identified and subsequently grouped in four categories of forcings: river flow (hydrological regime and discharge variability); tidal range (semimonthly and monthly tidal cycles); tidal cycles, and turbulence.

The relative influence of these forcings on turbidity variability varies along the estuarine axis and between the multiannual and seasonal time scales, exhibiting similar trends in the two estuaries. On multiannual time scale, the influence of river discharge increases toward upstream, from about 3% to 42-49%. In contrast, the contribution of tidal factors decreases up-estuary, from about 50% to 20% in the case of tidal cycles (from 15% to 6% for tidal range).

On seasonal time scale, turbidity in the lower estuary is dominated by tidal cycles, which explain 60% of turbidity variability, followed by tidal range and river flow. This pattern remains constant during both periods of high and low river discharge. By contrast, the dominant forcing at the upper estuary is tidal cycles during periods of low river discharge (explaining 50-60% of the turbidity variability), and river flow during periods of high river discharge (explaining up to about 70% of the turbidity variability).

This work has demonstrated that the evaluation of the forcings impact is an interesting tool to compare different estuaries throughout the world, in order to better understand their behavior and the common processes. The San Francisco Bay (USA) and the Blyth Estuary (UK) also showed a similar tidal contribution to the turbidity variability in lower reaches as that observed in the two French estuaries. However, the tidal range has a higher influence than the tidal cycles in the San Francisco Bay due to a local characteristic, i.e., the dependence of water slack durations on tidal range. The impact of river flow at the lower San Francisco Bay also is in concordance with the Gironde and Loire as the three systems have river discharges of the same order of magnitude. This suggests common patterns in the global influence of forcings on turbidity variability at lower reaches of estuaries dominated by both tides and river flow.

In a context of global change, identifying forcings affecting turbidity is not sufficient: the contribution of forcings to turbidity variability is also required. We propose that relative forcings contribution can be an appropriate indicator to quantify the long-term changes of forcings and their impact of suspended sediment. All this shows that the continuous record of turbidity in estuaries is recommended not only to evaluate the long-term variability of suspended sediment concentrations but also to quantify the weight of different environmental forcings on such variability. Other potential applications of the quantification and classification of forcings impact in environmental management include: forecast of future dredging strategies, prediction of the most affected estuarine region by climate change or by an operation as stored water release, estimation of the most appropriate frequencies for executing such water discharge, among others.

## **Acknowledgements**

I. Jalón-Rojas thanks the Agence de l'Eau Adour-Garonne (AEAG) and the Aquitaine Region for the financial support of her PhD grant. Authors gratefully acknowledge the MAGEST Consortium and the Groupement d'intérêt publique (GIP) Loire Estuary for providing turbidity time series. We address our sincere thanks to the three reviewers and to the guest editor who helped us to improve this article.



## References

- Alfieri, L., Burek, P., Feyen, L., Forzieri, G., 2015. Global warming increases the frequency of river floods in Europe. *Hydrol. Earth Syst. Sci.* 19, 2247–2260. doi:10.5194/hess-19-2247-2015
- Allen, G.P., Castaing, P., 1973. Suspended sediment transport from the Gironde estuary (France) onto the adjacent continental shelf. *Mar. Geol.* 14, 47–53.
- Allen, G.P., Salomon, J.C., Bassoullet, P., Du Penhoat, Y., De Grandpré, C., 1980. Effects of tides on mixing and suspended sediment transport in macrotidal estuaries. *Sediment. Geol.* 26, 69–90.
- Boé, J., Terray, L., Martin, E., Habets, F., 2009. Projected changes in components of the hydrological cycle in French river basins during the 21st century. *Water Resour. Res.* 45, W08426. doi:10.1029/2008WR007437
- Castaing, P., Allen, G.P., 1981. Mechanisms controlling seaward escape of suspended sediment from the Gironde: A macrotidal estuary in France. *Mar. Geol.* 40, 101–118.
- Castaing, P., Etcheber, H., Sottolichio, A., Cappe, R., 2006. Evaluation de l'évolution hydrodologique et sédimentaire du système Garonne-Dordogne-Gironde. Tech. rep., Rapport Agence de l'eau Adour-Garonne – Université de Bordeaux.
- Chernetsky, A.S., Schuttelaars, H.M., Talke, S.A., 2010. The effect of tidal asymmetry and temporal settling lag on sediment trapping in tidal estuaries. *Ocean Dyn.* 60, 1219–1241. doi:10.1007/s10236-010-0329-8
- Chevalier, L., Laignel, B., Massei, N., Munier, S., Becker, M., Turki, I., Coynel, A., Cazenave, A., 2013. Hydrological variability of major French rivers over recent decades, assessed from gauging station and GRACE observations. *Hydrol. Sci. J.* 59, 1844–1855. doi:10.1080/02626667.2013.866708
- Cheviet, C., Violeau, D., Guesmia, M., 2002. Numerical simulation of cohesive sediment transport in the Loire estuary with a three-dimensional model including new parameterisations, in: Winterwerp, J.C., Kranenburg, C. (Eds.), *Fine Sediment Dynamics in the Marine Environment*. Elsevier B.V., pp. 529–543.
- Daubechies, I., 1992. Ten Lectures on Wavelets, in: *IEEE Symposium on ComputerBased Medical Systems*. p. 357. doi:10.1137/1.9781611970104
- Derot, J., Schmitt, F.G., Gentilhomme, V., Zongo, S.B., 2015. Long-term high frequency phytoplankton dynamics, recorded from a coastal water autonomous measurement system in the eastern English Channel. *Cont. Shelf Res.* 109, 210–221. doi:10.1016/j.csr.2015.09.015
- Dyer, K.R., 1988. Fine sediment particle transport in estuaries, in: Dronkers, J., van Leussen, W. (Eds.), *Physical Process in Estuaries*. Springer-Verlag, pp. 427–445.
- Etcheber, H., Schmidt, S., Sottolichio, A., Maneux, E., Chabaux, G., Escalier, J.M., Wennekes, H., Derriennic, H., Schmeltz, M., Quéméner, L., Repecaud, M., Woerther, P., Castaing, P., 2011. Monitoring water quality in estuarine environments: lessons from the MAGEST monitoring programme in the Gironde fluvial-estuarine system. *Hydrol. Earth Syst. Sci.* 15, 831–840. doi:10.5194/hess-15-831-2011
- Farge, M., 1992. Wavelet transforms and their applications to turbulence. *Annu. Rev. Fluid Mech.* 24, 395. doi:10.1146/annurev.fluid.24.1.395

- Fettweis, M., Monbaliu, J., Baeye, M., Nechad, B., Van den Eynde, D., 2012. Weather and climate induced spatial variability of surface suspended particulate matter concentration in the North Sea and the English Channel. *Methods Oceanogr.* 3-4, 25–39. doi:10.1016/j.mio.2012.11.001
- French, J.R., Burningham, H., Benson, T., 2008. Tidal and Meteorological Forcing of Suspended Sediment Flux in a Muddy Mesotidal Estuary. *Estuaries and Coasts* 31, 843–859. doi:10.1007/s12237-008-9072-5
- Friedrichs, C.T., Aubrey, D.G., 1988. Non-linear tidal distortion in shallow well-mixed estuaries: a synthesis. *Estuar. Coast. Shelf Sci.* 27, 521–545. doi:10.1016/0272-7714(88)90082-0
- Gallenne, B., 1974. Les accumulations turbides de l'estuaire de la Loire. Etude de la crème de vase. University of Nantes.
- Ghil, M., Allen, M.R., Dettinger, M.D., Ide, K., Kondrashov, D., Mann, M.E., Robertson, A.W., Saunders, A., Tian, Y., Varadi, F., Yiou, P., 2002. Advanced spectral methods for climatic time series. *Rev. Geophys.* 40, 1003. doi:10.1029/2000RG000092
- GIP Groupement d'Intérêt Public Loire Estuaire, 2014. La dynamique du bouchon vaseux; Fiche L1.E2. GIP Loire Estuaire, Nantes, France.
- Grabemann, I., Uncles, R.J., Krause, G., Stephens, J.A., 1997. Behaviour of Turbidity Maxima in the Tamar (U.K.) and Weser (F.R.G.) Estuaries. *Estuar. Coast. Shelf Sci.* 45, 235–246. doi:10.1006/ecss.1996.0178
- Grinsted, a., Moore, J.C., Jevrejeva, S., 2004. Application of the cross wavelet transform and wavelet coherence to geophysical time series. *Nonlinear Process. Geophys.* 11, 561–566. doi:10.5194/npg-11-561-2004
- IPCC, 2013. *Climate Change 2013: The Physical Science Basis*. T.F. Stocker (Ed.) et al., Contribution of Working Group I to the Fifth Assessment Report of the Intergovernmental Panel on Climate Change. Cambridge University Press, Cambridge and New York.
- Jalón-Rojas, I., Schmidt, S., Sottolichio, A., 2016a. Evaluation of spectral methods for high-frequency multiannual time series in coastal transitional waters: advantages of combined analyses. *Limnol. Oceanogr. Methods* 14, Issue 6, 381–396.
- Jalón-Rojas, I., Schmidt, S., Sottolichio, A., 2015. Turbidity in the fluvial Gironde Estuary (southwest France) based on 10-year continuous monitoring: sensitivity to hydrological conditions. *Hydrol. Earth Syst. Sci.* 19, 2805–2819. doi:10.5194/hess-19-2805-2015
- Jalón-Rojas, I., Schmidt, S., Sottolichio, A., Bertier, C., 2016b. Tracking the turbidity maximum zone in the Loire Estuary (France) based on a long-term, high-resolution and high-frequency monitoring network. *Cont. Shelf Res.* 117, 1–11. doi:10.1016/j.csr.2016.01.017
- Le Hir, P., Thouvenin, B., 1994. Mathematical modelling of cohesive transport and particulate contaminants transport in the Loire estuary, in: Dyer, K.R., Orth, R.J. (Eds.), *Changes in Fluxes in Estuaries: Implications from Science to Management*. Olsen & Olsen, pp. 71–78.
- Lomb, N.R., 1976. Least-squares frequency analysis of unequally spaced data. *Astrophys. Space Sci.* 39, 447–462. doi:10.1007/BF00648343
- Mitchell S.B., Uncles R.J., Akesson L. 2012. Observations of turbidity in the Thames estuary. *Water and Environment Journal* 26, 511-520.

- Mitchell, S.B., Uncles, R.J., 2013. Estuarine sediments in macrotidal estuaries: Future research requirements and management challenges. *Ocean Coast. Manag.* 79, 97–100. doi:10.1016/j.ocecoaman.2012.05.007
- Press, W.H., Teukolsky, S., Vetterling, W.T., Flannery, B.P., 1992. *Numerical recipes in Fortran 77: the art of scientific computing*, Book. doi:10.1016/0378-4754(93)90043-T
- Pugh, D., 2004. *Changing Sea Levels: Effects of Tides, Weather and Climate*. Cambridge University Press.
- Robins, P.E., Skov, M.W., Lewis, M.J., Giménez, L., Davies, A.G., Malham, S.K., Neill, S.P., McDonald, J.E., Whitton, T.A., Jackson, S.E., Jago, C.F., 2016. Impact of climate change on UK estuaries: A review of past trends and potential projections. *Estuar. Coast. Shelf Sci.* 169, 119–135. doi:10.1016/j.ecss.2015.12.016
- Scargle, J.D., 1982. Studies in Astronomical Time-Series Analysis .2. Statistical Aspects of Spectral-Analysis of Unevenly Spaced Data. *Astrophys. J.* 263, 835–853. doi:10.1086/160554
- Schmidt S., Bernard C., Escalier J.-M., Etcheber E., Lamouroux M. (2016) Assessing and managing the risks of hypoxia in transitional waters: a case study in the tidal Garonne River (South-West France). *Environmental Science and Pollution Research*. doi:10.1007/s11356-016-7654-5
- Schmidt, S., Ouamar, L., Cosson, B., Lebleu, P., Derriennic, H., 2014. Monitoring turbidity as a surrogate of suspended particulate load in the Gironde Estuary: The impact of particle size on concentration estimates, in: *ISOBAY 2014*, abstract book, p. 17.
- Schmitt, F.G., 2008. Relating Lagrangian passive scalar scaling exponents to Eulerian scaling exponents in turbulence. *Eur. Phys. J. B* 48.
- Schmitt, F.G., Dur, G., Souissi, S., Brizard-Zongo, S., 2008. Statistical properties of turbidity, oxygen and pH fluctuations in the Seine river estuary (France). *Phys. A Stat. Mech. its Appl.* 387, 6613–6623. doi:10.1016/j.physa.2008.08.026
- Schoellhamer, D.H., 2002. Variability of suspended-sediment concentration at tidal to annual time scales in San Francisco Bay, USA. *Cont. Shelf Res.* 22, 1857–1866. doi:10.1016/S0278-4343(02)00042-0
- Schoellhamer, D.H., 2001. Singular spectrum analysis for time series with missing data. *Geophys. Res. Lett.* 28, 3187–3190.
- Schoellhamer, D.H., 1996. Factors affecting suspended-solids concentrations in South San Francisco Bay, California. *J. Geophys. Res.* 101, 87–95.
- Talke, S.A., de Swart, H.E., Schuttelaars, H.M., 2009. Feedback between residual circulations and sediment distribution in highly turbid estuaries: An analytical model. *Cont. Shelf Res.* 29, 119–135. doi:10.1016/j.csr.2007.09.002
- Torrence, C., Compo, G.P., 1998. A Practical Guide to Wavelet Analysis. *Bull. Am. Meteorol. Soc.* 79, 61–78. doi:10.1175/1520-0477(1998)079<0061:APGTWA>2.0.CO;2
- Uncles, R.J., Stephens, J.A., 1993. The Freshwater-Saltwater Interface and Its Relationship to the Turbidity Maximum in the Tamar Estuary, United Kingdom. *Estuaries*. doi:10.2307/1352770

- Uncles, R.J., Stephens, J.A., Harris, C., 2013. Towards predicting the influence of freshwater abstractions on the hydrodynamics and sediment transport of a small, strongly tidal estuary: The Devonshire Avon. *Ocean Coast. Manag.* 79, 83–96. doi:10.1016/j.ocecoaman.2012.05.006
- Uncles, R.J., Stephens, J.A., Law, D.J., 2006. Turbidity maximum in the macrotidal, highly turbid Humber Estuary, UK: Floccs, fluid mud, stationary suspensions and tidal bores. *Estuar. Coast. Shelf Sci.* 67, 30–52. doi:10.1016/j.ecss.2005.10.013
- Vautard, R., Yiou, P., Ghil, M., 1992. Singular-spectrum analysis: A toolkit for short, noisy chaotic signals. *Phys. D* 58, 95–126.
- Winterwerp, J.C., Wang, Z.B., 2013. Man-induced regime shifts in small estuaries—I: theory. *Ocean Dyn.* 63, 1279–1292. doi:10.1007/s10236-013-0662-9
- Zhang, M., Townend, I., Zhou, Y., Cai, H., 2016. Seasonal variation of river and tide energy in the Yangtze estuary, China. *Earth Surf. Process. Landforms* 41, 98–116. doi:10.1002/esp.3790